Available online at www.sciencedirect.com
ScienceDirect
Journal of Sound and Vibration 297 (2006) 727–742
JOURNAL OF SOUND AND VIBRATION
www.elsevier.com/locate/jsvi

On causality of the gradient elasticity models

A.V. Metrikine*

Faculty of Civil Engineering and Geosciences, Delft University of Technology, P.O. Box 5048, 2600 GA Delft, The Netherlands

Received 25 February 2005; received in revised form 30 March 2006; accepted 21 April 2006
Available online 21 June 2006

Abstract

This paper is concerned with causality of the gradient elasticity models of heterogeneous materials. As a rule, these models are not strictly causal since they allow an infinite speed of energy transfer by means of either propagating or transient evanescent waves. A discussion is presented in this paper of both physical and mathematical implications of this fact. This discussion is carried out employing one-dimensional (1D) second-order gradient models. A phenomenological enhancement is proposed, which makes these models causal. The main idea behind this enhancement is that a partial differential equation that governs dynamic behaviour of a causal gradient elasticity model *must* be of the same order with respect to spatial coordinate and with respect to time. The validity of this idea is confirmed in this paper by deriving a second-order 1D continuum model for concrete. A brief comparison is provided in conclusion of the equations of motion of the 1D second-gradient elasticity models and those used in dynamics of thin bars. It is shown that the proposed causal model corresponds to the most advanced dynamic models of such bars, namely to the Timoshenko model for the bending motion and the Mindlin model for the longitudinal motion of a bar.

1. Introduction

To approximate the mechanical behaviour of heterogeneous materials, generalized continuum models are often used, the general theories of which were developed by Mindlin [1], Green and Rivlin [2] and Suhubi and Eringen [3]. These models are homogeneous but more enhanced than the classical elastic continuum. The enhancement can be achieved via introduction of additional degrees of freedom (for example, of the rotational ones like in the Cosserat continuum [4]) or by accounting for the higher-order differential operators in the equations of motion (the so-called gradient elasticity models).

The generalized continua can accurately predict only those effects of heterogeneity, which correspond to the spatial scales at least a few times larger than the characteristic scale of heterogeneity. For example, a dependence of wave velocity of propagating waves on their frequency (the wave dispersion) can be predicted only of waves whose wavelength is sufficiently larger than the scale of heterogeneity. During the last decade,

*Corresponding author. Tel.: +0152784749;. fax: +152785767.
E-mail address: A.Metrikine@tudelft.nl.
URL: http://www.mechanics.citg.tudelft.nl/~andrei_m/.

0022-460X/$ - see front matter © 2006 Elsevier Ltd. All rights reserved.
doi:10.1016/j.jsv.2006.04.017

a number of papers were published on dynamic formulation of the generalized continua and on propagation of elastic waves in these continua. Particular attention in these papers was paid to (i) finding a comprehensive link between the underlying heterogeneity and the effective parameters of the generalized continua, (ii) reducing the number of non-classical parameters so that it would be feasible to measure these parameters, and (iii) studying propagation of high-frequency waves, the wavelength of which is comparable with the characteristic lengthscale of heterogeneity. These issues were addressed in the studies of Vardoulakis and Aifantis [5], Rubin et al. [6], Mühlhaus and Oka [7], Georgiadis et al. [8,9], Chen and Fish [10], Suiker et al. [11–13], Fish et al. [14,15], Andrianov [16], Wang and Sun [17], Askes et al. [18–20], Metrikine and Askes [21], Askes and Metrikine [22] Andrianov et al. [23].

The models proposed in the majority of the above-mentioned papers are stable and do ensure that the group velocity of propagating elastic waves has an upper limit thus satisfying the basic requirements of dynamic consistency. However, almost none of these models satisfy the Einstein's causality (also called strict causality [24,25]), which requires that no signal can travel faster than the velocity of light in vacuum. The majority of high-gradient models cited above do allow elastic energy to travel infinitely fast. This happens in spite of top-bounded group velocity of the propagating waves. The energy is transferred by means of evanescent (exponentially decaying with distance from a point of excitation) waves, which, very often, may exist in the generalized continua. Evanescent elastic waves can be observed in reality, while testing basically all heterogeneous materials. For example, in crystals (and in other periodically inhomogeneous materials) these waves occur if the excitation frequency belongs to the stop bands [26], within which waves experience resonance reflection. In disordered heterogeneous materials evanescent waves occur because of scattering on heterogeneities [27]. What, however, does not occur in reality but is predicted by many generalized continuum models (especially, by the gradient-elasticity models), is that evanescent waves may transfer elastic energy through a material instantly.

In this paper, an enhancement is proposed of the gradient elasticity models, which makes them causal (throughout this paper causality is understood in the original Einstein's sense). The basic idea behind this enhancement is that higher-order spatial gradients in gradient elasticity models must be accompanied by higher-order time derivatives. The validity of this idea is demonstrated in this paper by considering a 1D second-order gradient model. First, it is shown that by adding a higher-order time derivative (the fourth time derivative of displacement in this case) to the governing equation, the earlier derived models, such as in Refs. [8,21,22,28], can be made causal. Then, a continualization procedure developed in Refs. [22,28] is applied to a discrete chain of masses and springs, which is adopted as a 1D model of concrete on meso-level (two different types of masses and three different types of springs are used to mimic the aggregate, cement paste and interface fractions of concrete). Applying this procedure, a governing equation is derived for a second-order continuum, which contains fourth derivatives of displacement both with respect to time and the spatial coordinate. Thereby it is demonstrated that the presence of higher-order time derivatives is natural in a higher-order homogeneous continuum, which approximately describes a heterogeneous material.

This paper is structured as follows. In Section 2, a brief overview of 1D gradient elasticity models is presented and their dynamic properties are discussed. In Section 3, pulse-excitation and propagation of a plane wave in a gradient-elastic material is discussed. The material is described by a gradient elasticity model, which has a top-bounded group velocity of propagating waves. It is shown that this model is not causal and the reason of this non-causality is explained. In Section 4, a causal gradient elasticity model is introduced by adding a higher time derivative into the equation of motion. A discussion is provided, based on a dispersion analysis, as to why such introduction ensures causality. In Section 5, the causal model introduced in Section 4 is derived by continualizing equations of motion of a discrete chain of masses and springs. The elements of this chain are chosen such as to represent the meso-structure of concrete. In Section 6, a mathematical analogy is discussed between 1D gradient elasticity models and the models, which are used for predicting the longitudinal and transverse motions of a thin bar. It is shown that the causal model proposed in this paper is governed by equation of exactly the same form as the Timoshenko model for the transverse motion and the Mindlin model for the longitudinal motion of a thin bar.

2. Overview of 1D gradient elasticity models

All gradient elasticity models can be viewed as enhancements of the classical continuum. For the sake of clarity these enhancements will be presented and discussed shortly in this section on the hand of 1D second-order models. In accordance with the conventional terminology, the equations of motion for these models are partial differential equation of the order four with respect to the spatial coordinate. The only field variable in these equations is the longitudinal (codirected with the particle motion) displacement of the continua.

The simplest second-order model may be derived by a standard continualization of the equations of motion of a system of discrete particles [7,11,12,18] or by homogenizing a periodically inhomogeneous continuum taking into account its multiple spatial scales [10]. In 1D case the equation of motion for this model reads

$$u_{,tt} - c^2 u_{,xx} - c^2 l^2 A_{22} u_{,xxxx} = 0, \tag{1}$$

where $u(x,t)$ is the displacement of the continuum along the x-direction, t is the time, c is the classical wave speed, l is the lengthscale of the material heterogeneity, and A_{22} is a dimensionless positive parameter (model dependent).

The model governed by Eq. (1) can describe experimentally observed dispersive character of wave propagation in heterogeneous materials. However, this model suffers of a serious drawback: it is unstable at the short-wave domain [18,21]. Indeed, assuming that a harmonic wave of the form

$$u = U \exp(\mathrm{i}\omega t - \mathrm{i}kx) \tag{2}$$

propagates through the continuum described by Eq. (1), the following dispersion equation can be obtained

$$-\omega^2 + k^2 c^2 - k^4 l^2 c^2 A_{22} = 0. \tag{3}$$

It can be readily seen from Eq. (3) that as the wave number k exceeds the critical value $k_{\mathrm{cr}} = 1/\left(l\sqrt{A_{22}}\right)$, the angular frequency ω becomes imaginary, which corresponds to the exponential instability.

It is important to underline that the instability of short waves (shorter than the lengthscale) is physically acceptable for the model, Eq. (1), that is applicable only for waves, which are at least a few times longer than the characteristic lengthscale. However, mathematical analysis of Eq. (1) is considerably complicated by this instability.

There are a few possibilities to modify Eq. (1) so that the model becomes unconditionally stable without increasing the order of this equation. One modification was presented by Askes et al. [18]. It is based on a constitutive equation, which is used in gradient plasticity and gradient damage mechanics. This constitutive equation, as proposed on phenomenological grounds by Aifantis [29], in 1D case reads

$$\sigma = E(\varepsilon - l^2 \varepsilon_{,xx}), \tag{4}$$

where σ and ε are the axial stress and strain. In correspondence with this constitutive equation, the equation of motion, Eq. (1), was modified by Askes et al. [18] to

$$u_{,tt} - c^2 u_{,xx} + c^2 l^2 A_{22} u_{,xxxx} = 0 \tag{5}$$

which differs from Eq. (1) by just the sign of the last term (except the coefficient A_{22}, whose value may differ from that in Eq. (1) remaining, however, positive). Consequently, the dispersion equation, corresponding to Eq. (5) differs from Eq. (3) by the sign of the last term. Solving this dispersion equation, the following expressions can be found for the angular frequency and the group velocity of waves in the continuum modelled by Eq. (5):

$$\omega = \pm kc(1 + k^2 l^2 A_{22})^{1/2}, \quad c_{\mathrm{gr}} = \frac{\mathrm{d}\omega}{\mathrm{d}k} = \pm\, c\, \frac{1 + 2k^2 l^2 A_{22}}{(1 + k^2 l^2 A_{22})^{1/2}}. \tag{6}$$

The expression for the angular frequency shows that this frequency is real for all wavenumbers, which implies that the model is unconditionally stable. The expression for the group velocity, however, reveals that the shorter the waves (the larger the wavenumber k), the faster the elastic energy propagates through the continuum. The infinite energy propagation velocity (this equals in the case at hand to the group velocity) is also permitted by the model at infinitely short wavelengths. This can be considered as a drawback of the model

governed by Eq. (5), since it is unnatural that elastic waves may transfer energy infinitely fast. Let us underline once again, however, that application of basic physical principles to the model, which is supposed to work only for relatively long waves is questionable.

Another modification of Eq. (1) was derived by Fish et al. [14], by applying a homogenization technique to a periodically inhomogeneous continuum and taking into account both spatial and temporal scales. The equation of motion for the mean displacement obtained in Ref. [14] can be written as

$$u_{,tt} - c^2 u_{,xx} - l^2 A_{21} u_{,xxtt} = 0, \tag{7}$$

where A_{21} is a dimensionless positive parameter.

The dispersion equation for the model governed by Eq. (7) (which is obtained by assuming the travelling wave solution, Eq. (2)) reads

$$-\omega^2 + k^2 c^2 - \omega^2 k^2 l^2 A_{21} = 0. \tag{8}$$

On the basis of this equation, the following expressions can be found for the angular frequency and the group velocity

$$\omega = \pm \frac{kc}{(1 + k^2 l^2 A_{21})^{1/2}}, \quad c_{\mathrm{gr}} = \frac{c}{(1 + k^2 l^2 A_{21})^{3/2}}. \tag{9}$$

These expressions show that the model governed by Eq. (7) is unconditionally stable and propagating waves cannot transfer energy any quicker than with velocity c. The latter property of this model makes it superior to the model governed by Eq. (5). However, the model governed by Eq. (7) predicts that short waves transfer elastic energy with almost zero speed (as it follows from Eq. (9)). This is quite unrealistic.

It is natural to expect that a combination of the models governed by Eqs. (5) and (7) could also be derived. Such a model would include two higher order terms proportional to $u_{,xxxx}$ and $u_{,xxtt}$ and, as all the preceding models, would be a particular case of the general theory of Mindlin [1]. This model can indeed be found in the literature. It was used, for example, by Georgiadis et al. [8] and was derived from a discrete model by Metrikine and Askes [21], who employed a non-standard continualization procedure. The governing equation for this model can be written as

$$u_{,tt} - c^2 u_{,xx} - l^2 A_{21} \left(u_{,tt} - c^2 \frac{A_{22}}{A_{21}} u_{,xx} \right)_{,xx} = 0. \tag{10}$$

The angular frequency and the group velocity for this model can be found to depend on the wavenumber as

$$\omega = \pm kc \frac{(1 + k^2 l^2 A_{22})^{1/2}}{(1 + k^2 l^2 A_{21})^{1/2}}, \quad c_{gr} = \pm c \frac{1 + 2k^2 l^2 A_{22} + k^4 l^4 A_{21} A_{22}}{(1 + k^2 l^2 A_{21})^{3/2} (1 + k^2 l^2 A_{22})^{1/2}}. \tag{11}$$

These expressions show that the model is unconditionally stable and that propagating waves may transfer elastic energy with the speed, which equals c for long waves and $c(A_{22}/A_{21})^{1/2}$ for short waves. Thus, it may seem that the model governed by Eq. (10) is both stable and provides the lower and upper bounds for the speed of elastic energy transfer. The latter statement, however, is not quite correct. In spite of the bounded speed of energy transfer by *propagating* waves, the model does allow an infinite speed of elastic energy transfer by *evanescent* waves, thus suffering of non-causality. This issue is discussed in the following section.

3. Dynamic response to a pulse load

To demonstrate that the model governed by Eq. (10) is not causal, a transient dynamic response of a half-space, whose material is modelled by Eq. (10), to a uniform and normal pulse-loading applied to the surface is

considered in this section. The system of equations, which govern this response, is given as

$$\begin{aligned}
&u_{,\tau\tau} - u_{,\xi\xi} - A_{21}u_{,\xi\xi\tau\tau} + A_{22}u_{,\xi\xi\xi\xi} = 0, && \xi \geq 0, \quad \tau \geq 0,\\
&u(\xi, \tau = 0) = u_{,\tau}(\xi, \tau = 0) = 0, && \xi \geq 0,\\
&u_{,\xi\xi}(\xi = 0, \tau) = 0, && \tau \geq 0,\\
&\left(u_{,\xi} + A_{21}u_{,\xi\tau\tau} - A_{22}u_{,\xi\xi\xi}\right)_{\xi=0} = P\delta(\tau), && \tau \geq 0,\\
&\lim_{\xi\to\infty} u(\xi, \tau) = 0, && \tau < \infty,
\end{aligned} \tag{12}$$

where $\xi = x/l$ and $\tau = tc/l$ are the dimensionless coordinate normal to the half-space surface and dimensionless time, $P = F_0/(\rho c)$ (F_0 is the intensity density of the pulse with the dimension $\mathrm{N\,sm^{-2}}$), and $\delta(\tau)$ is the Dirac delta function. The boundary conditions in Eq. (12) are written in correspondence with the equation of motion, see Refs. [19,28].

The problem defined by Eq. (12) can be solved by applying the integral Laplace transform over the dimensionless time τ. Defining this transform as

$$U(\xi, s) = \int_0^\infty u(\xi, \tau)\exp(-s\tau)\,\mathrm{d}\tau \tag{13}$$

the following boundary-value problem is obtained in the Laplace domain

$$A_{22}U_{,\xi\xi\xi\xi} - U_{,\xi\xi}\left(1 - s^2A_{21}\right) + s^2U = 0 \quad \xi \geq 0, \tag{14}$$

$$\begin{aligned}
&U_{,\xi\xi}(\xi = 0, s) = 0,\\
&(U_{,\xi} + s^2A_{21}U_{,\xi} - A_{22}U_{,\xi\xi\xi})_{\xi=0} = P,
\end{aligned} \tag{15}$$

$$\lim_{\xi\to\infty} U(\xi, s) = 0 \quad \mathrm{Re}(s) > 0, \tag{16}$$

The general solution of Eq. (14), which satisfies the boundary condition at the infinity, Eq. (16), can be written as

$$U = C_1\exp(-k_1\xi) + C_2\exp(-k_2\xi), \tag{17}$$

where k_1 and k_2 are two of the four roots of the following characteristic equation

$$A_{22}k^4 + k^2(1 - s^2A_{21}) + s^2 = 0 \tag{18}$$

which satisfy the following condition: $\mathrm{Re}(k_{1,2}) > 0$ for $\mathrm{Re}(s) > 0$. These roots can be found analytically to give

$$k_{1,2} = (2A_{22})^{-1/2}\left(s^2A_{21} - 1 \pm \left((1 - s^2A_{21})^2 - 4s^2A_{22}\right)^{1/2}\right)^{1/2}. \tag{19}$$

The unknown constants C_1 and C_2 in Eq. (17) are found by substituting Eq. (17) into the boundary conditions at $\xi = 0$, Eq. (15), and then solving the obtained system of two linear algebraic equations. This completes solution of the problem in the Laplace domain. To return to the time domain the following inverse transform is to be applied:

$$u(\xi, \tau) = \frac{1}{2\pi\mathrm{i}}\int_{\gamma-\mathrm{i}\infty}^{\gamma+\mathrm{i}\infty} U(\xi, s)\exp(s\tau)\,\mathrm{d}s, \tag{20}$$

where $\mathrm{i} = (-1)^{1/2}$ and γ is real, positive and greater than the real part of all singularities of $U(\xi,s)$.

The inverse transform can be accomplished numerically by evaluating the following integral:

$$u(\xi, \tau) = \frac{1}{2\pi}\exp(\gamma\tau)\int_{-\omega_0}^{\omega_0} \mathrm{Re}(U(\xi, s = \gamma + \mathrm{i}\omega)\exp(\mathrm{i}\omega\tau))\,\mathrm{d}\omega, \tag{21}$$

where ω and ω_0 are real and the latter has a sufficiently large value for the integrand to vanish. The results of this evaluation, which was performed with $\gamma = 0.01$ and $\omega_0 = 200$, are shown in Fig. 1. The dimensionless coefficients were taken as $A_{21} = 1.78$ and $A_{22} = 0.34$. These values, as well as the value of $A_{23} = 0.66$ in the

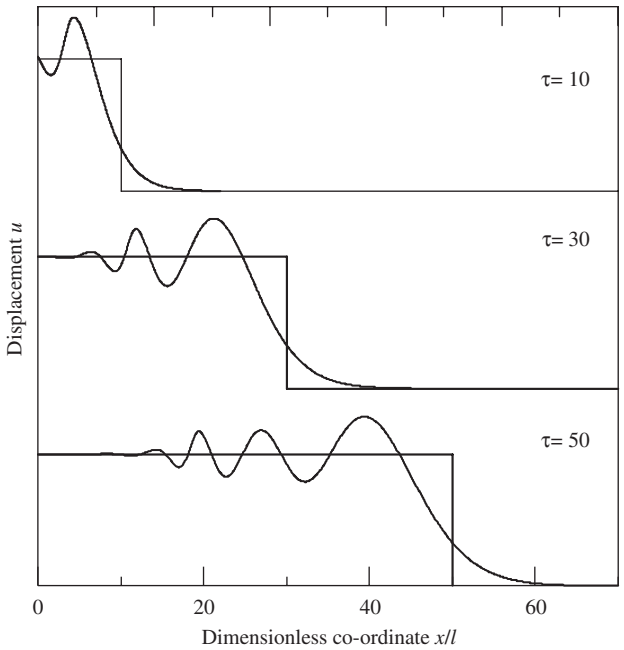

Fig. 1. Dynamic response of the non-causal model to a pulse-loading at three successive time moments.

forthcoming analysis, is not arbitrary. As will be shown in Section 5, these values correspond to a coarse-aggregated concrete.

Fig. 1 shows displacement $u(\xi,\tau)$ at three successive time moments. For comparison, at each time moment the corresponding displacement of the classical continuum model governed by the wave equation ($A_{12} = A_{22} = 0$) is also plotted in the figure. It can be seen from Fig. 1 that the elastic field propagating through the material has no sharp front. At any time instant, the material is disturbed not only behind but also before the classical wave front $\xi = \tau$. And, although the elastic field decays exponentially before the front, the following conclusion may be drawn from Fig. 1: the model at hand is not causal. The reason for the exponentially decaying 'messenger' to appear before the front is explained in Ref. [19]. What actually happens is that when a pulse propagates through the continuum, the elastic energy is carried by propagating waves, which have a finite propagation speed. However, every disturbed plane of the material generates not only propagating waves but also evanescent ones (one of the wavenumbers in Eq. (19) is real, whereas the other is imaginary once $s = i\omega$). These evanescent waves diffuse elastic energy instantly, thus serving as the reason for non-causality of the model.

In the next section, the model governed by Eq. (10) is enhanced by adding one term. It is shown that such addition makes the model causal and an explanation is given as to why this addition is natural. Later in this paper, the equation postulated in the next section will be derived from a discrete chain that represents the meso-structure of concrete.

4. The causal model postulated

To comply with Einstein's causality, a partial differential equation that governs dynamic behaviour of a 1D model *must* be of the same order with respect to the spatial coordinate and with respect to time. This necessary condition of causality has been proven for the second-order partial differential equations. The author is not aware of a proof of this condition for the higher-order equations. Therefore, in this paper this statement is just postulated.

Since Eq. (10) is of the order four with respect to the coordinate, the necessary condition of causality postulated above suggests that a term containing the fourth derivative over time should be added to this equation to make the model causal. It is important to realize that this term does not violate the second Newton

law, which says that an equation of motion must be of the second order with respect to time. One has to remember that this is applicable to *one* degree of freedom and *one* component of a material. Considering a heterogeneous material, one deals with at least two components. The motion of each component of the material has to be described by an equation of the second order with respect to time. However, once the decision has been made to model a heterogeneous material with the help of a homogenious model, the limitation of the order of the equation of motion with respect to time becomes groundless. On the contrary, it is natural to have this order equal to $2n \times N$, where n is the number of components of the material and N is the number of dimensions considered ($N = 1$ for 1D models).

The simplest possible term, which contains the fourth time derivative of the displacement, is $u_{,tttt}$ multiplied by a constant. Thus, the following modification of Eq. (10) may be expected to satisfy Einstein's causality:

$$u_{,tt} - c^2 u_{,xx} - l^2 A_{21}\left(u_{,tt} - c^2 \frac{A_{22}}{A_{21}} u_{,xx}\right)_{,xx} + \frac{l^2}{c^2} A_{23} u_{,tttt} = 0, \tag{22}$$

where A_{23} is a positive constant (it must be positive to avoid instability at infinitely long waves, which correspond to $u_{,xx} = u_{,xxxx} = 0$).

The dispersion equation corresponding to Eq. (22) reads

$$-\omega^2 + c^2 k^2 - l^2 A_{21} k^2 \left(\omega^2 - c^2 \frac{A_{22}}{A_{21}} k^2\right) + \frac{l^2}{c^2} A_{23} \omega^4 = 0. \tag{23}$$

When solved with respect to the angular frequency ω, the following *four* roots of this equation can be found

$$\omega = \pm c(2A_{23}l^2)^{-1/2}\left(1 + l^2 k^2 A_{21} \pm ((1 + l^2 k^2 A_{21})^2 - 4l^2 k^2 A_{23}(1 + l^2 k^2 A_{22}))^{1/2}\right)^{1/2}. \tag{24}$$

The model is stable if all four frequencies defined by Eq. (24) are real in the complete range of wavenumbers. This stability requirement imposes certain limitations on the parameters A_{21}, A_{22} and A_{23} because not all positive values of these parameters ensure stability.

Suppose that the parameters of the model are chosen such that the stability requirement is satisfied. In this case the dispersion curves visualizing the (ω,k) dependences given by Eq. (24) assume the shape shown in Fig. 2 by the solid lines. To plot this figure, the following values of the parameters were used: $A_{21} \approx 1.78$,

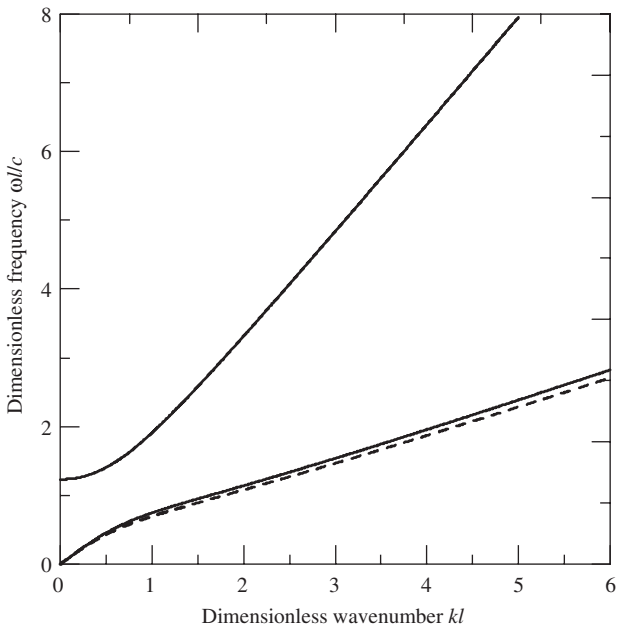

Fig. 2. Dispersion curves for the causal and non-causal models.

$A_{22} \approx 0.34$, $A_{23} \approx 0.66$. For comparison, the dispersion curve governed by Eq. (11) (non- causal model) is shown as the dashed line.

The qualitative difference between the models governed by Eq. (11) and Eq. (22) is the number of the branches of the dispersion curve. The improved model, Eq. (22), has two branches, whereas the non-causal model, Eq. (11), has only one. The second (high-frequency) branch of the dispersion curve is of crucial importance for causality of the model. Indeed, because of this branch, high-frequency (higher than the cut-off frequency of this branch) vibrations of an element of the continuum generate only propagating waves, whose propagation velocity is bounded. No evanescent waves, which 'diffuse' the elastic energy instantly is generated in this case. Thus, the high-frequency waves, which form the sharp front, propagate through the improved model with a finite speed. Thus, the model may be expected to comply with Einstein's causality. This expectation is confirmed in Fig. 3, where a snapshot of the displacement is shown of the half-space, which is excited by the pulse loading. This displacement was calculated following the same procedure as described in Section 3 (in fact, only the equation of motion should be changed in the statement Eq. (12) to Eq. (22)) and the same parameters as used for plotting the dispersion curves in Fig. 2.

The bold line in Fig. 3 shows the dimensionless displacement at the time instant $\tau = 10$ as predicted by the improved model. For comparison, the displacements are shown as calculated using the classical wave equation and the non-causal model, Eq. (11). Fig. 3 shows clearly that the improved model predicts a sharp front, which propagates somewhat faster than the classical wave front. The velocity of the front propagation can be easily calculated from Eq. (24) by taking the limit $k \to \infty$. This gives

$$c_{\max} = c(2A_{23})^{-1/2}\left(A_{21} + (A_{21}^2 - 4A_{23}A_{22})^{1/2}\right)^{1/2} \tag{25}$$

It may be noted from Fig. 3 that the displacement predicted by the non-causal and causal models, Eqs (11) and (22) differ perceptibly in spite of seemingly small difference between the governing equations introduced by the term proportional to fourth time derivative. This difference, however, is to be expected under the pulse loading and with no damping accounted for, since the models indeed differ at high-frequency band significantly. If an excitation was considered with the spectrum localized at a relatively low- frequency band (below the cut-off frequency of the upper dispersion branch in Fig. 2) or the material damping were accounted for, this difference would be hardly notable.

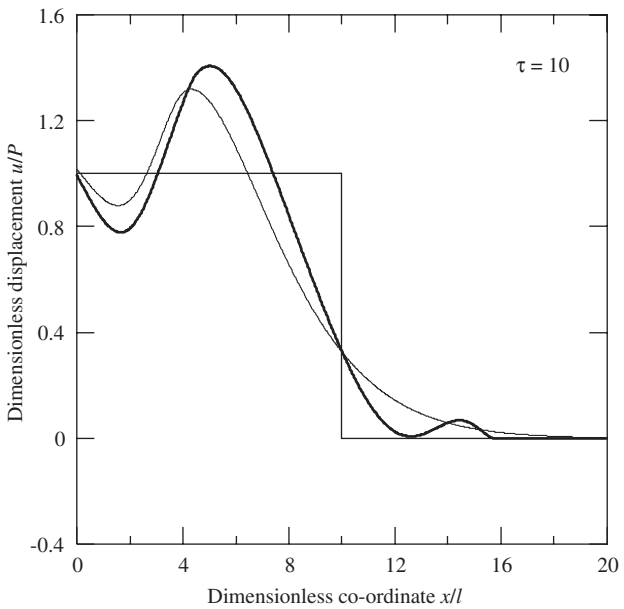

Fig. 3. Comparison of the dynamic responses of the causal and noon-causal models.

Thus, the proposed model, Eq. (22), is causal provided that the dimensionless parameters A_{21}, A_{22} and A_{23} are chosen properly. One of the best ways to do this is to derive Eq. (22) from a meso-structural representation of a heterogeneous material. This would allow to express A_{21}, A_{22} and A_{23} using the mechanical properties of the material components. In the next section such derivation is carried out starting from a discrete chain of masses and springs that simplistically represent the meso-structure of concrete.

5. Derivation of causal model from a discrete 1D model of concrete

Conventional concrete can be considered as the mixture of a relatively soft cement paste and a relatively stiff aggregate. Between these two fractions a thin interface exists, whose stiffness is even smaller than that of the cement paste [30]. The meso-structure of concrete is shown schematically at the upper part of Fig. 4. The black ovals in this figure represent the aggregate, the grey background represents the cement paste and the thin belts round the aggregate particles show the interface. The lower part of Fig. 4 shows a part of an infinite chain of masses and springs, which is adopted in this paper as a discrete 1D model of concrete. This chain is periodic (with a spatial period l) and contains two types of masses and three types of springs. The bigger black masses represent the inertial property of the aggregate, whereas the smaller grey masses represent that of the cement paste. The black, grey and light grey springs represent elasticity of the aggregate, cement paste, and interface, respectively.

The equations of motion that govern small longitudinal vibrations of the masses m_a and m_c about their equilibria can be written as

$$\begin{aligned} \ddot{x}_c^{(m)} + \omega_c^2\left(2x_c^{(m)} - x_c^{(m+1)} - x_c^{(m-1)}\right) + \omega_1^2\left(2x_c^{(m)} - x_a^{(m-1)} - x_a^{(m)}\right) = 0, \\ \ddot{x}_a^{(m)} + \omega_2^2\left(2x_a^{(m)} - x_c^{(m)} - x_c^{(m+1)}\right) = 0, \end{aligned} \tag{26}$$

where

$$\omega_1^2 = \omega_c^2 \frac{k_a k_i}{k_a k_c + k_a k_i + k_c k_i}, \quad \omega_2^2 = \omega_a^2 \frac{k_c k_i}{k_a k_c + k_a k_i + k_c k_i}, \quad \omega_a^2 = \frac{k_a}{m_a}, \quad \omega_c^2 = \frac{k_c}{m_c} \tag{27}$$

and $x_a^{(m)}(t)$ and $x_c^{(m)}(t)$ are the displacements of the masses m_a and m_c characterised by index (m).

To derive from Eq. (26) a partial differential equation, which would describe a stable and causal continuum, a continualization procedure should be applied that was proposed by Metrikine and Askes [21]. In accordance with this procedure, the displacements $x_a^{(m)}(t)$ and $x_c^{(m)}(t)$ of the masses of the chain should be related to the displacements $u_a(x,t)$ and $u_c(x,t)$ of a to-be-derived continuum non-locally (instead of using the conventional relations $x_a^{(m)}(t) = u_a(x,t)$ and $x_c^{(m)}(t) = u_c(x,t)$). Namely, the continuum displacements should be expressed as

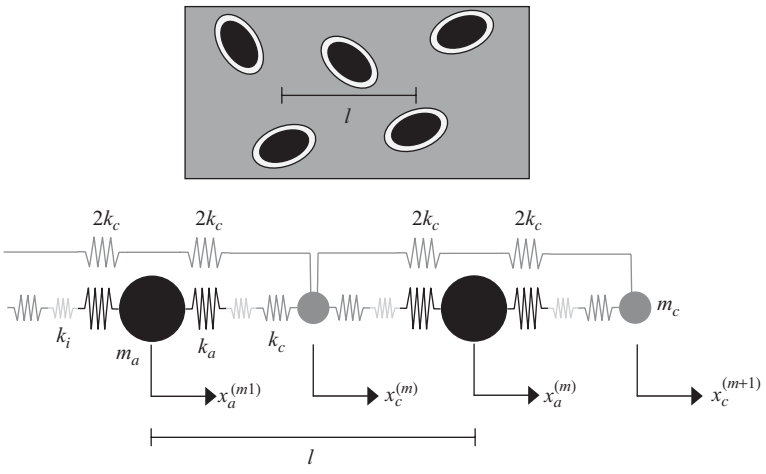

Fig. 4. Sketch of the meso-structure of concrete and a 1D chain of masses and springs that is adopted to represents this meso-structure.

weighted averages of the displacements of the masses of the same type that surround the central mass (m), i.e.

$$u_a(x,t)=\frac{1}{1+2a}\left(x_a^{(m)}+a\,x_a^{(m+1)}+a\,x_a^{(m-1)}\right),\quad u_c(x,t)=\frac{1}{1+2a}\left(x_c^{(m)}+ax_c^{(m+1)}+ax_c^{(m-1)}\right),\tag{28}$$

where a is a dimensionless weighting coefficient, which has to be not smaller than zero and smaller than unity.

To continualize the chain (or, mathematically speaking, to convert the ordinary differential equations with finite difference equations, Eq. (26), to a partial differential equation), the kinematic relations, Eq. (28), are to be inverted to give explicit expressions for the displacements of the masses $x_a^{(m)}(t)$ and $x_c^{(m)}(t)$ through the continuum displacements. This inversion can be carried out by assuming that the differences $x_{a,c}^{(m)}(t)=u_{a,a}(x,t)$ are small, so that the following relation holds

$$x_{a,c}^{(m)}=u_{a,c}(x,t)+\sum_{k=1}^{2N}l^k f_{a,c}^{(k)}(x,t)+O(L^{2N+1}),\tag{29}$$

where l is the spatial period of the chain, N is the order of the to-be-derived continuum and $f_{a,c}(x,t)$ are unknown deviation functions, which have to be derived in correspondence with Eq. (28). The differential operator $L=l\partial/\partial x$ in Eq. (29) should be much smaller than unity in the sense that the result of application of this operator to a function should be much smaller that the function itself. To enable convergence of the series in Eq. (29), it is sufficient that the deviation functions $f_{a,c}(x,t)$ satisfy the following inequality:

$$l^{k+1}\left|f_{a,c}^{(k+1)}\right|\ll q_{a,c}l^k\left|f_{a,c}^{(k)}\right|,\quad q_{a,c}<1.\tag{30}$$

To find explicit expressions for the deviation functions, the displacements $x_{a,c}^{(m)}(t)$ and the displacements of the neighbour masses $x_{a,c}^{(m\pm1)}(t)$ are to be substituted into the kinematic relations, Eq. (28). The latter displacements can be derived using Eq. (29) via the Taylor series expansions. This results in the following expression:

$$\begin{aligned}x_{a,c}^{(m\pm1)}&=u_{a,c}(x\pm l,t)+\sum_{k=1}^{2N}l^k f_{a,c}^{(k)}(x\pm l,t)+O(L^{2N+1})\\&=\sum_{j=0}^{2N}(\pm l)^j\frac{1}{j!}\frac{\partial^j u_{a,c}(x,t)}{\partial x^j}+\sum_{k=1}^{2N}l^k\sum_{j=0}^{2N}(\pm l)^j\frac{1}{j!}\frac{\partial^j f_{a,c}(x,t)}{\partial x^j}+O(L^{2N+1}).\end{aligned}\tag{31}$$

Substituting Eqs. (29) and (31) into the kinematic relations, Eq. (28), and setting each multiplier of a power of l to zero separately, a set of recurrence relations can be obtained, ordered by corresponding powers of l. The first five equations of this set, which are relevant for this development, are shown below

$$\begin{aligned}l^0:&\quad u_{a,c}=u_{a,c},\\l^1:&\quad 0=f_{a,c}^{(1)},\\l^2:&\quad 0=f_{a,c}^{(2)}+\tfrac{a}{1+2a}\tfrac{\partial^2 u_{a,c}}{\partial x^2},\\l^3:&\quad 0=f_{a,c}^{(3)}+\tfrac{a}{1+2a}\tfrac{\partial^2 f_{a,c}^{(1)}}{\partial x^2},\\l^4:&\quad 0=f_{a,c}^{(4)}+\tfrac{a}{12(1+2a)}\tfrac{\partial^4 u_{a,c}}{\partial x^4}+\tfrac{a}{1+2a}\tfrac{\partial^2 f_{a,c}^{(2)}}{\partial x^2}.\end{aligned}\tag{32}$$

Eqs. (32) show that the odd-order deviation functions $f_{a,c}^{(j)},\ j=1,3,5\ldots$ are zero. All even-order deviation functions can be expressed as linear, even-order differentials of $u_{a,c}$.

With the deviation functions known, Eqs. (29) and (31) can be substituted into the equations of motion of the masses of the chain, Eq. (26). This substitution results in the equations of motion of a gradient continuum. To derive a second-order continuum ($N=2$), these equations are to be truncated to the order 4 of the spatial period l. Before truncating, however, the classical continuum parameters (Young's moduli $E_{a,c,i}$ and material densities $\rho_{a,c}$) should be introduced instead of the stiffnesses $k_{a,c,i}$ and masses $m_{a,c}$. In the 1D case under consideration the relations between these quantities read

$$\rho_{a,c}=m_{a,c}/l^3,\quad E_{a,c,i}=k_{a,c,i}/l.\tag{33}$$

Consequently, and in accordance with Eq. (27), parameters ω_c^2, ω_1^2 and ω_2^2 in Eq. (35) and (36) can be expressed as

$$\omega_1^2 = L^2 c_1^2, \quad \omega_2^2 = L^2 c_2^2, \quad c_1^2 = c_c^2 \frac{E_a E_i}{E_a E_c + E_a E_i + E_c E_i}, \quad c_2^2 = c_a^2 \frac{E_c E_i}{E_a E_c + E_a E_i + E_c E_i}, \tag{34}$$

where $c_c = \sqrt{E_c/\rho_c}$ and $c_a = \sqrt{E_a/\rho_a}$ are the wave speeds in the cement paste and the aggregate, respectively.

Now the truncation can be accomplished to give a system of two partial differential equations with respect to $u_a(x,t)$ and $u_c(x,t)$:

$$\begin{aligned}
&\frac{l^4}{1+2a}\left\{(c_c^2(1+2a)+2a\omega_1^2)\frac{(10a-1)}{12(1+2a)}\frac{\partial^4 u_c}{\partial x^4} - a\frac{\partial^4 u_c}{\partial x^2 \partial t^2} - c_1^2\frac{(10a-1)(2a-1)}{24(1+2a)}\frac{\partial^4 u_a}{\partial x^4}\right\}\\
&- l^3 c_1^2 \frac{4a-1}{6(1+2a)}\frac{\partial^3 u_a}{\partial x^3} + l^2\left\{\frac{\partial^2 u_c}{\partial t^2} - \frac{1}{1+2a}(c_c^2(1+2a)+2ac_1^2)\frac{\partial^2 u_c}{\partial x^2} + c_1^2\frac{2a-1}{2(1+2a)}\frac{\partial^2 u_a}{\partial x^2}\right\}\\
&+ lc_1^2\frac{\partial u_a}{\partial x} + 2c_1^2(u_c - u_a) = 0,
\end{aligned} \tag{35}$$

$$\begin{aligned}
&\frac{l^4}{1+2a}\left\{ac_2^2\frac{(10a-1)}{6(1+2a)}\frac{\partial^4 u_a}{\partial x^4} - a\frac{\partial^4 u_a}{\partial x^2 \partial t^2} - c_2^2\frac{(10a-1)(2a-1)}{24(1+2a)}\frac{\partial^4 u_c}{\partial x^4}\right\}\\
&+ l^3 c_2^2 \frac{4a-1}{6(1+2a)}\frac{\partial^3 u_c}{\partial x^3} + l^2\left\{\frac{\partial^2 u_a}{\partial t^2} - c_2^2\frac{2a}{1+2a}\frac{\partial^2 u_a}{\partial x^2} - c_2^2\frac{2a-1}{2(1+2a)}\frac{\partial^2 u_c}{\partial x^2}\right\}\\
&- lc_2^2\frac{\partial u_c}{\partial x} + 2c_2^2(u_a - u_c) = 0
\end{aligned} \tag{36}$$

Each of the above two equations is of the second order with respect to time, which complies with second Newton law in the sense that each degree of freedom of a mechanical system is governed by an equation that contains the mass times acceleration term and no higher time derivatives.

To obtain from Eqs. (35) and (36) a single equation, which could be compared to Eq. (22), one may apply the following procedure. First, the integral Fourier transforms, which are defined as

$$U_{a,c}(k,\omega) = \int_{-\infty}^{\infty}\int_{-\infty}^{\infty} u_{a,c}(x,t)\exp(-\mathrm{i}\omega t + \mathrm{i}kx)\,\mathrm{d}x\,\mathrm{d}t \tag{37}$$

are applied to Eqs. (35) and (36). By applying these transforms, a system of two following linear algebraic equations is obtained:

$$\begin{aligned}
a_{11}U_a + a_{12}U_c = 0,\\
a_{21}U_a + a_{22}U_c = 0,
\end{aligned} \tag{38}$$

where

$$\begin{aligned}
a_{11} = {}& \frac{l^4}{1+2a}\left\{\left(c_c^2(1+2a)+2a\omega_1^2\right)\frac{(10a-1)}{12(1+2a)}k^4 - a\omega^2 k^2\right\}\\
&+ l^2\left\{-\omega^2 + \frac{1}{1+2a}\left(c_c^2(1+2a)+2ac_1^2\right)k^2\right\} + 2c_1^2,
\end{aligned}$$

$$\begin{aligned}
a_{12} = {}& -\frac{l^4 c_1^2 k^4}{1+2a}\frac{(10a-1)(2a-1)}{24(1+2a)} - l^3 c_1^2 ik^3\frac{4a-1}{6(1+2a)} - l^2 c_1^2 k^2\frac{2a-1}{2(1+2a)} - lc_1^2 ik - 2c_1^2,\\
a_{21} = {}& -\frac{l^4 c_2^2 k^4}{1+2a}\frac{(10a-1)(2a-1)}{24(1+2a)} + l^3 c_2^2 ik^3\frac{4a-1}{6(1+2a)} + l^2 c_2^2 k^2\frac{2a-1}{2(1+2a)} + lc_2^2 ik - 2c_2^2,\\
a_{22} = {}& \frac{l^4}{1+2a}\left\{ac_2^2\frac{(10a-1)}{6(1+2a)}k^4 - a\omega^2 k^2\right\} + l^2\left\{-\omega^2 + c_2^2\frac{2a}{1+2a}k^2\right\} + 2c_2^2.
\end{aligned} \tag{39}$$

Setting the determinant of the coefficient matrix of this system to zero results in the following dispersion equation:

$$a_{11}a_{22} - a_{12}a_{21} = 0. \tag{40}$$

Analysing the expressions for a_{ij}, Eq. (39), it is easy to see that this dispersion equation contains terms with the order of l up to l^8. To make the dispersion equation, Eq. (40), consistent with the adopted accuracy $O(L^5)$, it has to be truncated by cutting off all terms which are of the order higher than l^4. This simplifies Eq. (40) to the dispersion equation of the model, which was postulated in the previous section, Eq. (23):

$$-\omega^2 + c^2k^2 - l^2A_{21}k^2\left(\omega^2 - c^2\frac{A_{22}}{A_{21}}k^2\right) + \frac{l^2}{c^2}A_{23}\omega^4 = 0. \tag{41}$$

The coefficients of this equation, however, are now known and are expressed through the material parameters of concrete as

$$\begin{gathered} c^2 = \tfrac{c_2^2}{2}\tfrac{c_1^2+2c_c^2}{c_1^2+c_2^2}, \quad A_{21} = \tfrac{c_c^2}{2(c_1^2+c_2^2)} + \tfrac{2a}{(1+2a)}, \\ A_{22} = \tfrac{22a-1}{12(1+2a)}, \quad A_{23} = \tfrac{c_2^2}{4}\tfrac{c_1^2+2c_c^2}{(c_1^2+c_2^2)^2}. \end{gathered} \tag{42}$$

Because of uniqueness of the Fourier transforms, dispersion equation, Eq. (41), can be used to retrieve the corresponding equation of motion. This can be done by using the following symbolic relations between the frequencies and wavenumbers and corresponding time and space derivatives:

$$-\omega^2 \leftrightarrow \partial^2/\partial t^2, \quad \omega^4 \leftrightarrow \partial^4/\partial t^4, \quad -k^2 \leftrightarrow \partial^2/\partial x^2, \quad k^4 \leftrightarrow \partial^4/\partial x^4.$$

Using these relations the following equation of motion is obtained from Eq. (41)

$$u_{,tt} - c^2u_{,xx} - l^2A_{21}\left(u_{,tt} - c^2\frac{A_{22}}{A_{21}}u_{,xx}\right)_{,xx} + \frac{l^2}{c^2}A_{23}u_{,tttt} = 0, \tag{43}$$

where $u(x,t)$ is an effective deflection of the continuum. Obviously Eqs. (43) and (22) (the latter was postulated in the previous section) are the same.

It is interesting to note that Eq. (43) describes a more consistent second-order continuum than the system of Eqs. (35) and (36), from which it was derived. Indeed, Eq. (43) describes a causal, unconditionally stable continuum, while one can easily check that Eqs. (35) and (36) describe a continuum that suffers from both short-wave instability and non-causality. This seemingly strange fact has a clear explanation. The point is that neither Eq. (43) nor Eqs. (35)–(36) are supposed to describe accurately dynamic processes, of which the wavelength is shorter than required by the adopted accuracy $O(L^5)$. And it is precisely at these wavelengths that the deviation between the two statements becomes apparent and the instability, as well as non-causality, occurs. What makes Eq. (43) superior to the system of Eqs. (35) and (36) is that it takes into account all terms, which satisfy accuracy $O(L^5)$ and only these terms. On the contrary, Eqs. (35)–(36) contain terms up to accuracy $O(L^9)$ but far not all of them, which makes this system inconsistent.

As mentioned above, the major advantage of deriving governing equations for a higher-order continuum from a meso-structural representation of a heterogeneous material (relative to a phenomenological formulation of these equations) is that the coefficients of the derived equations are known in terms of physical parameters of the material components. In the case at hand, this concerns coefficients c, A_{21}, A_{22} and A_{23}, which are expressed through the parameters of the aggregate, cement paste and interface in Eq. (42). The only unknown parameter in these equations is the weighting parameter a. Let us define it for a specific case taking example of a coarse-aggregated concrete.

Suppose that the paste occupies $v_c = 40\%$ of the representative volume of a concrete specimen and, consequently, the aggregate occupies $v_a = 60\%$ of this volume (the volumetric fraction of the interface is usually negligible). The Young's modulus and mass density of the paste and aggregate, as well as the Young's modulus of the interface, depend of the type of concrete. Here, the following figures are adopted:

$$E_c = 23\,\mathrm{GPa}, \;\; E_a = 40\,\mathrm{GPa}, \;\; E_i = 7\,\mathrm{GPa}, \;\; \rho_c = 2162\,\mathrm{kg\,m^{-3}}, \;\; \rho_a = 2691\,\mathrm{kg\,m^{-3}}. \tag{44}$$

Substitution of these values into Eq. (42) gives

$$c \approx 2286\,\mathrm{m\,s^{-1}}, \quad A_{21} \approx 1.348 + \frac{2a}{(1+2a)}, \quad A_{22} = \frac{22a-1}{12(1+2a)}, \quad A_{23} \approx 0.66. \tag{45}$$

To identify the weighting coefficient a, one can make use of Eq. (25), which gives an expression for the maximum velocity of energy propagation in the continuum as a function of the above parameters. This velocity, on the other hand, can be easily estimated as

$$c_{\max} = \frac{v_a + v_c}{v_a/c_a + v_c/c_c} \approx 3594\,\mathrm{m\,s^{-1}}, \tag{46}$$

where $c_c = \sqrt{E_c/\rho_c} \approx 3262\,\mathrm{m\,s^{-1}}$ and $c_a = \sqrt{E_a/\rho_a} \approx 3855\,\mathrm{m\,s^{-1}}$ are the wave speeds in the cement paste and aggregate, respectively.

Substituting c, A_{21}, A_{22} and A_{23} given by Eq. (45) and the value of $c_{\max}$ given by Eq. (46) into Eq. (25), one obtains an algebraic equation with respect to a. This equation can be shown to have only one root in the interval $0 \leqslant a \leqslant 1$, which is given as

$$a \approx 0.374. \tag{47}$$

With this weighting coefficient, Eq. (45) results in the following values, which were used throughout this paper:

$$c \approx 2286\,\mathrm{m\,s^{-1}}, \quad A_{21} \approx 1.78, \quad A_{22} \approx 0.34, \quad A_{23} \approx 0.66. \tag{48}$$

Finalizing this section, let us underline its two major results. The first result is that a procedure has been developed of theoretical identification of the relationships between the material properties of the fractions of the original heterogeneous material and the effective parameters of the corresponding (approximate) second-order continuum model. The second and, probably, more general result is that the presence of the fourth time-derivative of the displacement in the equation of motion for a second-order gradient continuum *naturally* follows from an accurate continualization procedure of an originally heterogeneous model. This is a strong argument that supports the main idea of this paper that the gradient elasticity models should satisfy the Einstein's causality.

6. Mathematical analogy with models for longitudinal and transverse vibrations of a homogeneous bar

The 1D gradient-elasticity models of heterogeneous materials, which have been discussed in the preceding sections, have one-to-one mathematical analogues in the theories of both the longitudinal and transverse vibrations of homogeneous thin bars. These analogues are briefly discussed in this section with the aim to show that the causal model, Eq. (22), corresponds mathematically to the most advanced 1D dynamic models.

Consider a thin bar with a circular cross section, which is made of a homogeneous material and axially tensioned. The longitudinal $u(x,t)$ and transverse $w(x,t)$ free motions of a differential element of this bar can be most roughly described by the following wave equations [31]:

$$\rho u_{,tt} - E u_{,xx} = 0, \tag{49}$$

$$\rho A w_{,tt} - T w_{,xx} = 0, \tag{50}$$

where ρ and E are the mass density and Young's modulus of the bar material, A is the cross-sectional area and T is the axial tension.

Eqs. (49) and (50) are valid under a number of assumptions, which allow to neglect the dispersive character of wave propagation in the bar. To derive Eq. (49), the uniform stress distribution over the cross section must be assumed and the lateral inertia should be unaccounted for. Similarly, to derive Eq. (50), one has to neglect the bending stiffness of the bar, as well as the shearing effects. In what follows, these assumptions are gradually abandoned and the resulting models are compared to those discussed in the preceding sections. The order of the comparison is chosen to follow the discussion of the gradient elasticity models in Sections 2 and 3.

It seems that there are no models for a thin homogeneous bar, which are governed by Eq. (1). Most likely, this is because of the stability requirement, the violation of which is unacceptable in structural

mechanics. Eq. (5), however, is mathematically analogues to the following well-known equation [31]

$$\rho A w_{,tt} - T w_{,xx} + EI w_{,xxxx} = 0, \tag{51}$$

which describes the transverse motion of a tensioned bar (a beam) in accordance with the Euler–Bernoulli assumptions. Eq. (51) differs from Eq. (50) by the last term, which takes into account the bending stiffness EI of the bar (I is the moment of inertia of the cross section).

The form of Eq. (7) coincides with the following equation

$$\rho u_{,tt} - E u_{,xx} - \rho v^2 \kappa^2 u_{,xxtt} = 0, \tag{52}$$

which governs the longitudinal motion of the bar, once its lateral inertia is accounted for (the Rayleigh–Love theory). In Eq. (52), v is the Poison's ratio and κ^2 is the polar radius of gyration [31].

Eq. (10) is analogues to that, which governs the transverse motion of the tensioned bar in correspondence with the Rayleigh theory, which extends the Euler–Bernoulli assumptions by accounting for the rotary-inertia effects. The latter equation reads

$$\rho A w_{,tt} - T w_{,xx} + EI w_{,xxxx} - \rho I w_{,xxtt} = 0. \tag{53}$$

In the theory of structural vibrations it is known (see Refs. [31,32]) that all models introduced in this section, Eqs. (49)–(53) cannot correctly describe even the first mode (with respect to the lateral coordinate) of the bar vibrations at relatively high frequencies. To improve this, Timoshenko has proposed an enhanced theory for the transverse motion of the bar, while Mindlin has done it for the longitudinal motion. The governing equations for both these models have the same form (the physical background and the meaning of coefficients are, of course, totally different). Therefore, to avoid unnecessary repetitions, only the governing equation resulting from the Timoshenko theory is shown here. Taking into account the tensile force, this equation can be written as [31]

$$\rho A w_{,tt} - T w_{,xx} + EI\left(1 + \frac{T}{GAk}\right) w_{,xxxx} - \rho I\left(1 + \frac{E}{Gk} + \frac{T}{GAk}\right) w_{,xxtt} + \frac{\rho^2 I}{Gk} w_{,tttt} = 0, \tag{54}$$

where κ is the Timoshenko shear coefficient and G is the shear modulus.

Comparing Eq. (54) to Eq. (22), one can see that these equations have identical form. The same form would accept the governing equation of the Mindlin theory if written as a single equation. Thus, the causal gradient-elastic model proposed in this paper corresponds mathematically to the best- known models describing the dispersive character of wave propagation in 1D systems. This is an additional argument supporting the model proposed in this paper.

7. Discussion and conclusions

Einstein's causality principle requires that no signal can propagate faster than the light speed in vacuum. This is one of the most fundamental principles of modern physics, and any general model, which is supposed to be applicable at the complete frequency band, must satisfy it. All researchers agree with this statement. Many models, however, are designed to work only at a specific frequency band. Homogeneous continuum elasticity models, for example, are *all* applicable only at a relatively low-frequency band (at which the lengthscale of corresponding mechanical processes is much larger than the characteristic length of the material microstructure). Should such models satisfy Einstein's causality? There is no consensus among researchers as to how to answer this question in the case that non-causality is associated with the frequency band at which the model in question is not applicable according to its original assumptions.

The author of this paper advocates the following answer to the above stated question. Imagine two models of a material, which, with the same accuracy, describe dynamic behaviour of the material at a desired frequency band. Imagine further that one model is causal whereas the other is not causal but its non-causality is associated with the frequencies outside the considered frequency band. In this case, the causal model should be preferred. Not only should it be done because it complies with Einstein's causality. More importantly, causal models profit from applicability of Kramers–Kronig relations [33,34] (a logical consequence of causality [24]), which strictly relate the dispersive and dissipative properties of materials. These relations are

widely applied for experimental identification of material properties. Not as a logical argument but definitely as one worth mentioning, one should realize that the most classical models of continuum mechanics such as the classical elastic continuum and Cosserat continuum do comply with Einstein's causality.

In this paper, causality of gradient elasticity models has been discussed. It has been shown that the majority of these models are not causal as they allow elastic energy either to travel with an infinite speed or to diffuse instantly. A brief overview has been given of existing second-order gradient elasticity models in 1D.

A causal 1D second-order gradient elasticity model has been proposed. First, the equation of motion of this model has been postulated on the basis of a general idea that in order to comply with Einstein's causality, higher-order spatial gradients in gradient elasticity models must be accompanied by higher-order time derivatives. Then, this equation has been derived by continualizing a discrete chain of masses and springs. The composition of this chain has been chosen to represent the meso-structure of concrete. The applied continualization procedure has allowed to relate the material properties of the fractions of the original heterogeneous material and the effective parameters of the corresponding gradient elasticity model. Additionally, it has shown that the causal gradient elasticity model *naturally* results from accurate continualization of originally heterogeneous material model.

A dispersion analysis of the derived causal model has shown that at a relatively low-frequency band, at which the homogeneous gradient elasticity models are applicable, the derived causal model is almost identical to the most advanced, though non-causal, model known in literature. Thus, both these models are equivalent in the desired frequency band but the causal model should be preferred because of above formulated reasons.

To strengthen this conclusion, a mathematical analogy has been investigated between the 1D gradient elasticity models and the models used in dynamics of thin rods. The proposed causal model has been shown to be governed by equation of exactly the same form as the governing equations of the Timoshenko-beam model and Mindlin-rod model, which are known to be the most advanced models for the thin rods.

References

[1] R.D. Mindlin, Micro-structure in linear elasticity, *Archive for Rational Mechanics and Analysis* 16 (1964) 51–78.

[2] A.E. Green, R.S. Rivlin, Multipolar continuum mechanics, *Archive for Rational Mechanics and Analysis* 17 (1964) 113–147.

[3] E.S. Suhubi, A.C. Eringen, Nonlinear theory of micro-elastic solids—II, *International Journal of Engineering Science* 2 (1964) 389–404.

[4] E. Cosserat, F. Cosserat, *Théorie des Corps Deformables*, Herman et fils, Paris, 1909.

[5] I. Vardoulakis, E.C. Aifantis, On the role of microstructure in the behavior of soils: effects of higher order gradients and internal inertia, *Mechanics of Materials* 18 (1994) 151–158.

[6] M.B. Rubin, P. Rosenau, O. Gottlieb, Continuum model of dispersion caused by an inherent material characteristic length, *Journal of Applied Physics* 77 (1995) 4054–4063.

[7] H.B. Mühlhaus, F. Oka, Dispersion and wave propagation in discrete and continuous models for granular materials, *International Journal of Solids and Structures* 33 (1996) 2841–2858.

[8] H.G. Georgiadis, I. Vardoulakis, G. Lykortafitis, Torsional surface waves in a gradient-elastic half-space, *Wave Motion* 31 (2000) 333–348.

[9] H.G. Georgiadis, E.G. Velgaki, High-frequency Rayleigh waves in materials with micro-structure and couple-stress effects, *International Journal of Solids and Structures* 40 (2003) 2501–2520.

[10] W. Chen, J. Fish, A dispersive model for wave propagation in periodic heterogeneous media based on homogenization with multiple spatial and temporal scales, *ASME Journal of Applied Mechanics* 68 (2001) 153–161.

[11] A.S.J. Suiker, R. de Borst, C.S. Chang, Micro-mechanical modelling of granular material—part 1: derivation of a second-gradient micro-polar constitutive theory, *Acta Mechanica* 149 (2001) 161–180.

[12] A.S.J. Suiker, R. de Borst, C.S. Chang, Micro-mechanical modelling of granular material—part 2: plane wave propagation in infinite media, *Acta Mechanica* 149 (2001) 161–180.

[13] A.S.J. Suiker, A.V. Metrikine, R. de Borst, Comparison of wave propagation characteristics of the Cosserat continuum and corresponding discrete lattice models, *International Journal of Solids and Structures* 38 (2001) 1563–1583.

[14] J. Fish, W. Chen, G. Nagai, Non-local dispersive model for wave propagation in heterogeneous media: one-dimensional case, *International Journal for Numerical Methods in Engineering* 54 (2002) 331–346.

[15] J. Fish, W. Chen, G. Nagai, Non-local dispersive model for wave propagation in heterogeneous media: multi-dimensional case, *International Journal for Numerical Methods in Engineering* 54 (2002) 347–363.

[16] I.V. Andrianov, The specific features of the limiting transition from a discrete elastic medium to a continuous one, *Journal of Applied Mathematics and Mechanics* 66 (2002) 261–265.

[17] Z.P. Wang, C.T. Sun, Modeling micro-inertia in heterogeneous materials under dynamic loading, *Wave Motion* 36 (2002) 473–485.

[18] H. Askes, A.S.J. Suiker, L.J. Sluys, A classification of higher-order strain-gradient models—linear analysis, *Archive of Applied Mechanics* 72 (2002) 171–188.
[19] H. Askes, A.V. Metrikine, One-dimensional dynamically consistent gradient elasticity models derived from a discrete microstructure—part 2: static and dynamic response, *European Journal of Mechanics A/Solids* 21 (2002) 573–588.
[20] H. Askes, A.V. Metrikine, Higher-order continua derived from discrete media: continualisation aspects and boundary conditions, *International Journal of Solids and Structures* 42 (2005) 187–202.
[21] A.V. Metrikine, H. Askes, One-dimensional dynamically consistent gradient elasticity models derived from a discrete microstructure—part 1: generic formulation, *European Journal of Mechanics A/Solids* 21 (2002) 555–572.
[22] H. Askes, A.V. Metrikine, One-dimensional dynamically consistent gradient elasticity models derived from a discrete microstructure—part 2: static and dynamic response, *European Journal of Mechanics A/Solids* 21 (2002) 573–588.
[23] I.V. Andrianov, J. Awrejcewicz, R.G. Barantsev, Asymptotic approaches in mechanics: new parameters and procedures, *ASME Applied Mechanics Reviews* 56 (2003) 87–110.
[24] J.S. Toll, Causality and the dispersion relation: logical foundations, *Physical Review* 104 (1956) 1760–1770.
[25] H. Nussenzveig, *Causality and Dispersion Relations*, Academic Press, New York, 1972.
[26] L. Brillouin, M. Parodi, *Propagation des ondes dans les milieux périodiques*, Masson, Dunod, Paris, 1956.
[27] P. Sheng, *Scattering and Localization Of Classical Waves In Random Media*, World Scientific, Singapore, 1990.
[28] A.V. Metrikine, H. Askes, An isotropic dynamically consistent gradient elasticity model derived from a 2D lattice, *Philosophical Magazine A* 86 (2006) 3259–3286.
[29] E.C. Aifantis, Gradient deformation models at nano, *micro, and macro scales, ASME Journal of Engineering Materials and Technology* 121 (1999) 189–202.
[30] G. Lilliu, J.G.M. van Mier, 3D lattice type fracture model for concrete, *Engineering Fracture Mechanics* 70 (2003) 927–941.
[31] K.F. Graff, *Wave Motion In Elastic Solids*, Oxford University Press, London, 1975.
[32] H. Kolsky, *Stress Waves in Solids*, Dover, New York, 1963.
[33] R.D.L. Kronig, On the theory of the dispersion of X-rays, *Journal of the Optical Society of America and Review of Scientific Instruments* 12 (1926) 547–557.
[34] H.A. Kramers, La difusion de la lumiere par les atomes, *Estratto dagi Atti del Congresso Internazionaledi Fisici Como* 2 (1927) 545–557.